



## Research article

# Cardiac transcriptomic changes induced by early CKD in mice reveal novel pathways involved in the pathogenesis of Cardiorenal syndrome type 4

Francisco Javier Munguia-Galaviz<sup>a,b</sup>, Yanet Karina Gutierrez-Mercado<sup>c</sup>, Alejandra Guillermina Miranda-Diaz<sup>a</sup>, Eliseo Portilla de Buen<sup>d</sup>, Mario Eduardo Flores-Soto<sup>e</sup>, Raquel Echavarría<sup>f,\*</sup>

<sup>a</sup> Departamento de Fisiología, CUCS, Universidad de Guadalajara, Guadalajara 44340, Jalisco, Mexico

<sup>b</sup> División de Ciencias de la Salud, CUSUR, Universidad de Guadalajara, Ciudad Guzman 49000, Jalisco, Mexico

<sup>c</sup> Departamento de Clínicas, CUALTOS, Universidad de Guadalajara, Tepatitlan 47620, Jalisco, Mexico

<sup>d</sup> División de Investigación Quirúrgica, Centro de Investigación Biomedica de Occidente, Instituto Mexicano del Seguro Social, Guadalajara 44340, Mexico

<sup>e</sup> División de Neurociencias, Centro de Investigación Biomedica de Occidente, Instituto Mexicano del Seguro Social, Guadalajara 44340, Jalisco, Mexico

<sup>f</sup> CONAHCYT-Centro de Investigación Biomedica de Occidente, Instituto Mexicano del Seguro Social, Guadalajara 44340, Jalisco, Mexico

## ARTICLE INFO

## Keywords:

Cardiorenal  
Transcriptomics  
mRNA  
Heart  
Kidney  
Uropathy  
CKD

## ABSTRACT

**Background:** Cardiorenal syndrome (CRS) type 4 is prevalent among the chronic kidney disease (CKD) population, with many patients dying from cardiovascular complications. However, limited data regarding cardiac transcriptional changes induced early by CKD is available.

**Methods:** We used a murine unilateral ureteral obstruction (UUO) model to evaluate renal damage, cardiac remodeling, and transcriptional regulation at 21 days post-surgery through histological analysis, RT-qPCR, RNA-seq, and bioinformatics.

**Results:** UUO leads to significant kidney injury, low uremia, and pathological cardiac remodeling, evidenced by increased collagen deposition and smooth muscle alpha-actin 2 expression. RNA-seq analysis identified 76 differentially expressed genes (DEGs) in UUO hearts. Upregulated DEGs were significantly enriched in cell cycle and cell division pathways, immune responses, cardiac repair, inflammation, proliferation, oxidative stress, and apoptosis. Gene Set Enrichment Analysis further revealed mitochondrial oxidative bioenergetic pathways, autophagy, and peroxisomal pathways are downregulated in UUO hearts. Vimentin was also identified as an UUO-upregulated transcript.

**Conclusions:** Our results emphasize the relevance of extensive transcriptional changes, mitochondrial dysfunction, homeostasis deregulation, fatty-acid metabolism alterations, and vimentin upregulation in CRS type 4 development.

\* Corresponding author. CONAHCYT-Centro de Investigación Biomedica de Occidente, Instituto Mexicano del Seguro Social. Sierra Mojada 800 Independencia, Guadalajara 44340, Mexico.

E-mail address: [rechavarría@conacyt.mx](mailto:rechavarría@conacyt.mx) (R. Echavarría).

<https://doi.org/10.1016/j.heliyon.2024.e27468>

Received 21 August 2023; Received in revised form 26 December 2023; Accepted 29 February 2024

Available online 8 March 2024

2405-8440/© 2024 The Authors. Published by Elsevier Ltd. This is an open access article under the CC BY-NC license (<http://creativecommons.org/licenses/by-nc/4.0/>).

## 1. Introduction

Cardiorenal syndrome (CRS) encompasses acute and chronic pathophysiological interactions between the cardiovascular and renal systems [1]. In the case of CRS type 4, primary chronic kidney disease (CKD) results in chronic heart failure (HF) [2]. Hemodynamic changes, neurohumoral disturbances, anemia, mineral metabolism disorders, and uremic toxins are some of the mechanisms that converge in CRS, complicating its understanding [1,3].

CKD affects more than 10% of the general population worldwide and is a significant cause of mortality [4]. Cardiovascular disease (CVD) is more prevalent among the CKD population, with many patients dying from CVD complications [5–8]. Hence, understanding the pathophysiological processes associated with CKD and its cardiac consequences is vital to improving the prevention, diagnosis, and treatment of CRS type 4.

Left-ventricular hypertrophy and fibrosis are frequently associated with uremia in end-stage renal disease (ESRD) patients heavily burdened by CVD [9]. However, there is evidence of pathological cardiac performance and remodeling occurring early in CKD when the renal dysfunction is mild [10–13].

Transcriptome profiling is valuable for discovering biomarkers and therapeutic targets. Nevertheless, the number of transcriptomic studies in experimental models of CRS remains limited. Here, we explored the cardiac transcriptomic changes in an early-stage CKD murine model induced by unilateral ureteral obstruction (UUO) and identified novel pathways involved in the pathogenesis of CRS type 4. Our results suggest that early CKD can lead to the onset of widespread transcriptional changes implicated in CVD development.

## 2. Method and materials

### 2.1. Animals

8–12-week-old male C57BL/6 mice were housed in our local animal facility with free access to water and a standard rodent diet. All animal care and research methods followed institutional and federal regulations (NOM-062-200-1999), the ARRIVE guidelines, and the National Research Council's Guide for the Care and Use of Laboratory Animals. The Local Health Research Committee of CIBO, IMSS (CLIES R-2021-1305-013) approved all the procedures.

### 2.2. Murine model of UUO

The UUO surgery was previously described [14]. We performed a midline incision in mice ( $N = 5$ ) under xylazine (10 mg/kg)/ketamine (100 mg/kg) i.m. anesthesia to expose, ligate, and cut the left ureter before closing the midline incision. A sham group ( $N = 5$ ) underwent the same procedures except for ureter ligation. Cardiac blood, kidneys, and heart were collected under anesthesia on day 21 post-surgery. Tissues were fixed in 4% paraformaldehyde or immediately frozen and stored at  $-80^{\circ}\text{C}$ .

### 2.3. Renal function

Serum was obtained by centrifugation at  $3500 \times g$  for 15 min at  $4^{\circ}\text{C}$ . We determined serum creatinine (sCR) and blood urea nitrogen (BUN) levels with kits (Valtek Diagnostics, Santiago, Chile) according to the manufacturer's protocols. The absorbances were recorded with an EPOCH spectrophotometer (BioTek, Winooski, VT, USA). The mRNA expression of the injury marker neutrophil gelatinase-associated lipocalin (*Ngal*) was determined by RT-PCR.

### 2.4. RT-qPCR

RNA was isolated from the whole kidney and heart with Trizol (Invitrogen, Carlsbad, CA). The RevertAid First Strand cDNA Synthesis Kit (Thermo Fisher Scientific, Waltham, MA, USA) was used to synthesize cDNA. RT-qPCR was performed in a QuantStudio™ 5 instrument (Thermo Fisher Scientific, Waltham, MA, USA) with Green-2-Go-qPCR-Mastermix-ROX (BioBasic, Markham, ON, Canada) and the primers listed in Supplementary\_Table\_S1. We used the delta-CT method to determine gene expression differences normalizing with the glyceraldehyde 3-phosphate dehydrogenase (*Gapdh*) gene.

### 2.5. Histological analysis

Paraffin-embedded 5- $\mu\text{m}$  slices were dewaxed, rehydrated, and stained with hematoxylin and eosin (H&E), periodic acid-Schiff (PAS), and Sirius red. For immunohistochemistry, we used citrate buffer (10 mM, pH6.0) for antigen retrieval and the peroxidase-based Novolink Polymer Detection System (Leica Biosystems, Wetzlar, Germany) with polyclonal primary antibodies against smooth muscle alpha-actin 2 (ACTA2) and vimentin (VIM) (CST, Danvers, MA, US). Images were recorded in a DMi1 light microscope at 400X (Leica, Wetzlar, Germany) and quantified in NIH ImageJ/Fiji software.

### 2.6. Library construction and RNA sequencing (RNA-seq)

We performed RNA-seq to investigate mRNA expression profiles of male murine hearts 21 days after UUO surgery ( $N = 3$ ) vs. sham ( $N = 3$ ). First, a poly(A) RNA-seq library was prepared following Illumina's TruSeq-stranded-mRNA sample preparation protocol

(Illumina, San Diego, CA, USA) after passing RNA integrity checks (RIN>7) in an Agilent Technologies 2100 Bioanalyzer (Agilent, Santa Clara, CA, USA). Poly(A) tail-containing mRNAs were purified using oligo-(dT) magnetic beads. Poly(A) RNA was fragmented at high temperatures in a divalent cation buffer. Quality control and sequencing library quantification were performed using Agilent Technologies 2100 Bioanalyzer High Sensitivity DNA Chip. Paired-ended sequencing was performed on Illumina's NovaSeq 6000 system (LC Sciences, Houston, TX, USA). The raw sequence data have been submitted to NCBI Gene Expression Omnibus (GEO) repository under accession code GSE235751.

## 2.7. Bioinformatic analysis

### 2.7.1. Transcripts Assembly

Low-quality reads were removed with Cutadapt v1.10 and in-house perl scripts. We verified sequence quality with FastQC 0.10.1 (<http://www.bioinformatics.babraham.ac.uk/projects/fastqc/>) and used HISAT2 2.0 to map reads to [ftp://ftp.ensembl.org/pub/release-101/fasta/mus\\_musculus/dna/genome](ftp://ftp.ensembl.org/pub/release-101/fasta/mus_musculus/dna/genome). The mapped reads of each sample were assembled using StringTie. All transcriptomes were merged to reconstruct a comprehensive transcriptome using perl scripts and gffcompare (<https://github.com/gpertea/gffcompare>).

### 2.7.2. Differential expression analysis of mRNAs

We used StringTie 1.3.4 and ballgown (<http://www.bioconductor.org/packages/release/bioc/html/ballgown.html>) to estimate expression levels by calculating Fragments Per Kilobase per Million (FPKM). mRNAs differential expression analysis was performed by R package DESeq2 between two different groups (and by R package edgeR between two samples). mRNAs with a false discovery rate (FDR) < 0.05 and absolute fold-change  $\geq 2$  were considered differentially expressed genes (DEGs).

### 2.7.3. DEGs enrichment analysis

We used the Gene Ontology (GO) project (<http://www.geneontology.org>) and enrichment analysis for functional interpretation of the RNA-seq experimental data. The Kyoto Encyclopedia of Genes and Genomes (KEGG) (<http://www.kegg.jp/>) was used to identify the significant pathways (P < 0.05) associated with enriched DEGs. Gene Set Enrichment Analysis (GSEA) (<https://www.gsea-msigdb.org/gsea/index.jsp>) was used to identify pathways in which several genes change a small amount but in a coordinated way [15]. Gene sets with  $|NES| \geq 1$ , NOM p-val < 0.05, and FDR q-val < 0.25 are considered significant.

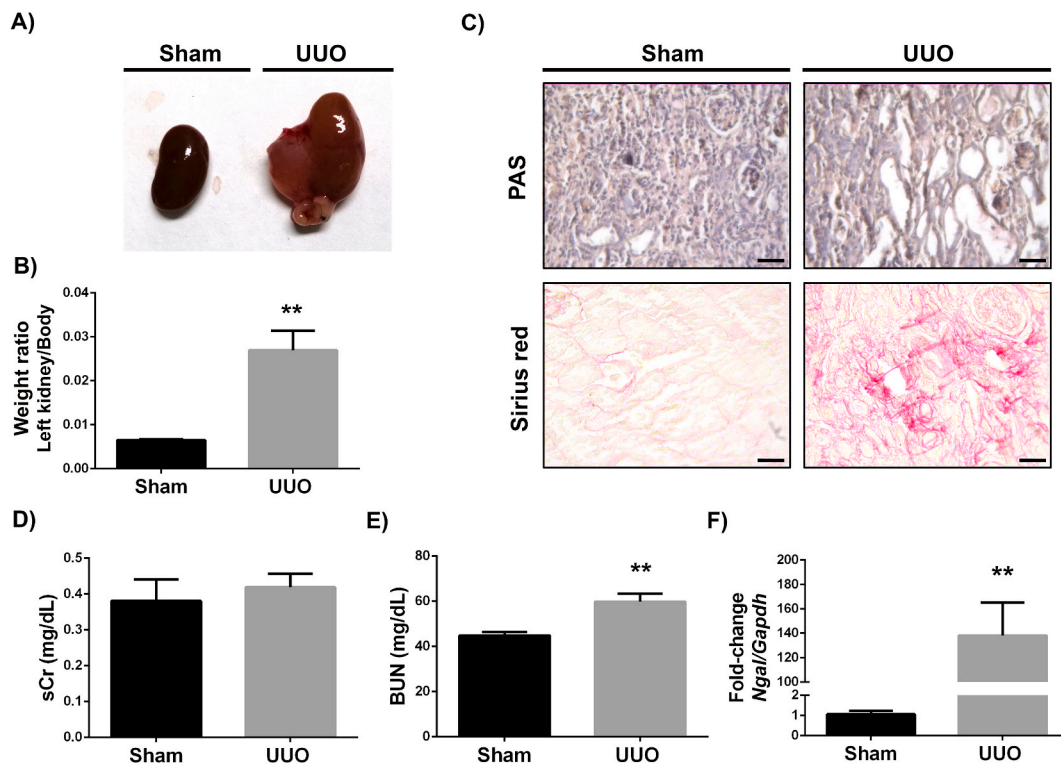


**Fig. 1. Kidney injury post-UUO.** (A) Sham and UUO kidneys representative images. (B) Left kidney weight/Bw ratio. (C) Histological analysis of sham and UUO kidneys with PAS and Sirius red (400X, scale bar = 100 μm). Levels of (D) sCr (mg/dL) and (E) BUN (mg/dL). (F) *Ngal/Gapdh* fold-change by RT-qPCR. N = 5, \*\*P < 0.005.

## 2.8. Statistical analysis

Data are presented as mean  $\pm$  SEM. We used the Mann-Whitney *U* test and Spearman's correlation for comparisons between two groups of non-parametric data and correlation analysis, respectively.  $P \leq 0.05$  was considered statistically significant. Analyses were done in GraphPad Pro (GraphPad, San Diego, CA).

## 3. Results

### 3.1. UUO as an early CKD model

UUO resulted in significant hydronephrosis at day 21 post-surgery (Fig. 1A), and the left kidney weight/body weight ratio is higher compared to sham (Fig. 1B). Histological analysis of the obstructed kidneys indicated the presence of tubular dilation, cast formation, and extracellular matrix deposition (Fig. 1C). Despite the significant damage observed in UUO mice, sCR levels were undistinguishable from sham (Fig. 1D), whereas BUN presented a slight but significant ( $P < 0.05$ ) increase (Fig. 1E). In contrast, *Ngal* expression in the obstructed kidneys had a  $>130$ -fold change increase ( $P < 0.005$ ) (Fig. 1F). At 21 days post-UUO, mice experience severe damage in the obstructed kidney. Yet, the intact contralateral kidney allows this model to be mildly uremic, thus making it valuable for studying early CKD.

### 3.2. Pathological remodeling in UUO hearts

Previously, Ham O et al. reported cardiac hypertrophy and increased mRNA expression of the hypertrophy-associated genes in UUO mice at 21 days post-surgery [12]. However, we did not observe an increment in heart weight/BW ratio nor significant changes in gene expression for atrial natriuretic peptide (*Anp*) and brain natriuretic peptide (*Bnp*) in UUO animals vs. sham (Fig. 2A–C). Still, UUO induced pathological cardiac remodeling, as evidenced by increased collagen deposition and ACTA2 expression (Fig. 2D and E). These results correlate with previous reports of fibrosis development in the hearts of UUO animals that have been associated with early activation of the Transforming Growth Factor beta (TGF- $\beta$ )/Smad signaling pathway [12,16].

### 3.3. DEGs in UUO hearts

Next, we investigated mRNA expression profiles of male murine hearts 21 days after UUO surgery vs. sham. Fig. 3A shows a box

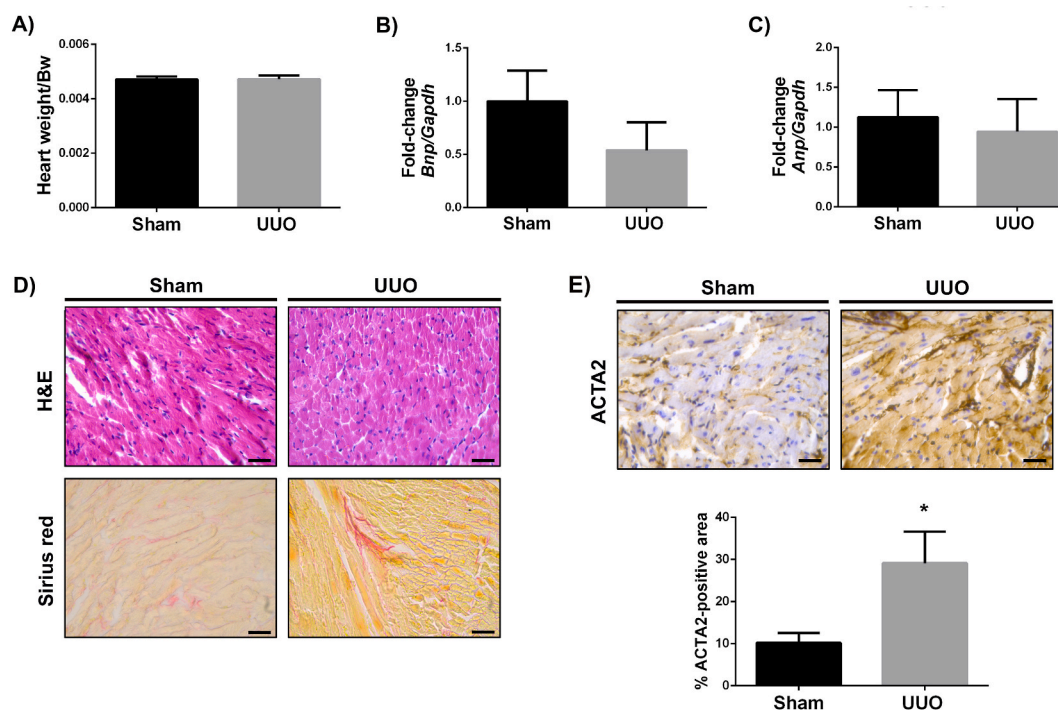


**Fig. 2. Pathological remodeling in UUO hearts.** (A) Heart weight/Bw ratio. (B) *Bnp/Gapdh* fold-change by RT-qPCR. (C) *Anp/Gapdh* fold-change by RT-qPCR. (D) Histological analysis of sham and UUO hearts with H&E and Sirius red, and (E) ACTA2 immunohistochemical detection and quantification (400X, scale bar = 100  $\mu$ m). N = 5, \* $P < 0.05$ .

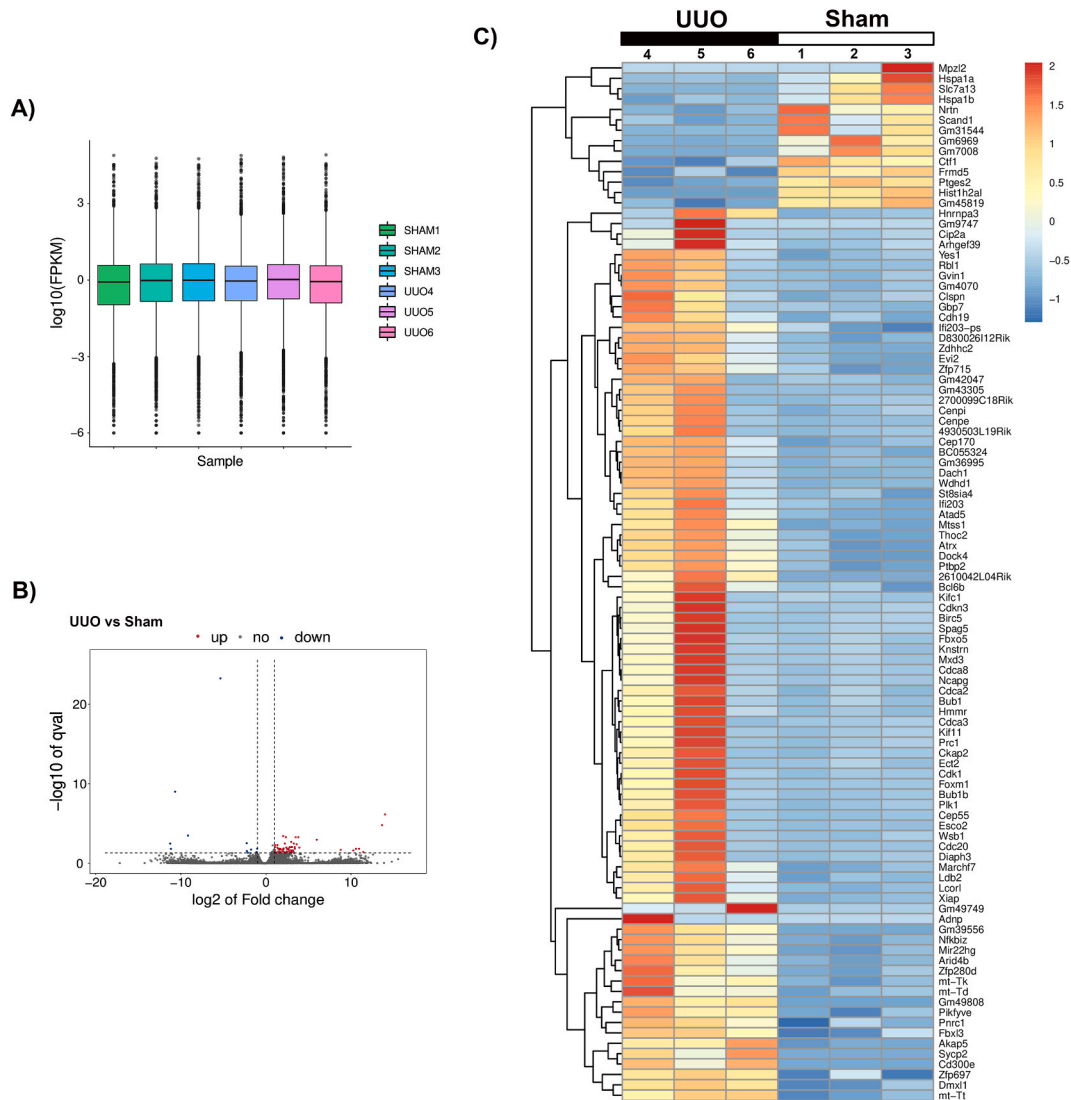


**Fig. 3. DEGs in UUO hearts.** (A) Box plot of  $\log_2(\text{FPKM})$  values. (B) Volcano map showing the distribution of DEGs in UUO vs. sham hearts. (C) Heatmap plot of DEGs. Red = upregulated and blue = downregulated.  $P < 0.05$  and  $\log_2$  (fold change)  $> 1$ .  $N = 3$ .

plot of  $\log_2(\text{FPKM})$  values across UUO and sham-expressed transcripts. RNA-seq identified 99 DEGs with a  $\log_2$  (fold-change) $>1$ . Among these, 76 DEGs (65 upregulated and 11 downregulated) were significantly and differentially expressed ( $P < 0.05$ ) between UUO and sham hearts (Supplementary\_file\_1). The most relevant differentially expressed mRNAs are shown in Table 1. A volcano map reflects the distribution of DEGs (Fig. 3B), and a heatmap analysis illustrates DEG’s expression pattern differences between experimental groups and replicates (Fig. 3C).

### 3.4. Upregulated DEGs are enriched in cell cycle and cell division pathways

GO analysis of DEGs in UUO hearts revealed significant enrichment in 10 GO terms within three independent categories: biological process (46), cellular component (49), and molecular function (4) (Supplementary\_file\_2). The 50 most enriched GO terms ( $P < 0.05$ ) are shown in Fig. 4A. Also, a scatterplot of the top enriched 20 GO terms indicates that several upregulated genes are enriched in cell cycle, cell division, spindle, midbody, anaphase-promoting complex binding, mitotic cytokinesis, chromosome-centromere, kinetochore, and spindle pole (Fig. 4B).

KEGG pathway analysis further revealed 29 different pathways in UUO hearts vs. sham, but only 4 were statistically significant ( $P < 0.05$ ) (Supplementary\_file\_2). Consistently with the GO analysis, the cell cycle was a significantly enriched pathway along with oocyte meiosis, progesterone-mediated oocyte maturation, and spliceosome (Fig. 4C).

**Table 1**  
Differentially expressed cardiac mRNAs in UUO vs. sham.

Gene	Description	Fold-change	P-value	Expression
Slc7a13	solute carrier family 7, member 13	0.000	1.87E-06	down
Hist1h2al	histone cluster 1, H2al	0.001	7.53E-14	down
Mpzl2	myelin protein zero-like 2	0.002	6.22E-08	down
Nrtn	neurturin	0.209	1.37E-06	down
Scand1	SCAN domain-containing 1	0.211	5.61E-05	down
Ctfl	cardiotrophin 1	0.231	1.45E-04	down
Frmf5	FERM domain containing 5	0.463	1.02E-04	down
Ptges2	prostaglandin E synthase 2	0.490	1.67E-05	down
Zfp715	zinc finger protein 715	2.002	6.92E-05	up
Ldb2	LIM domain binding 2	2.084	1.22E-04	up
Thoc2	THO complex 2	2.102	7.26E-06	up
Bcl6b	B cell CLL/lymphoma 6, member B	2.121	9.53E-05	up
Yes1	YES proto-oncogene 1, Src family tyrosine kinase	2.211	1.29E-04	up
St8sia4	ST8 alpha-N-acetylneuraminide alpha-2,8-sialyltransferase 4	2.252	1.35E-04	up
Cdh19	cadherin 19, type 2	2.293	1.58E-04	up
Lcor1	ligand dependent nuclear receptor corepressor-like	2.408	1.16E-04	up
Nfkbiz	nuclear factor of kappa light polypeptide gene enhancer in B cells inhibitor, zeta	2.544	3.27E-06	up
Akap5	A kinase (PRKA) anchor protein 5	2.551	1.06E-05	up
Zdhhc2	zinc finger, DHHC domain containing 2	2.785	6.22E-05	up
Gbp 7	guanylate binding protein 7	2.833	1.02E-04	up
Wsb1	WD repeat and SOCS box-containing 1	3.057	9.04E-05	up
Ifi203-ps	interferon activated gene 203, pseudogene	3.071	2.81E-05	up
Gvin1	GTPase, very large interferon inducible 1	3.271	2.12E-05	up
Wdhd1	WD repeat and HMG-box DNA binding protein 1	3.466	8.17E-05	up
Zfp697	zinc finger protein 697	3.988	6.59E-05	up
Dach1	dachshund family transcription factor 1	4.083	8.33E-08	up
Cdc20	cell division cycle 20	4.152	2.68E-05	up
Plk1	polo like kinase 1	4.567	1.09E-04	up
Evi 2	ecotropic viral integration site 2	4.666	1.73E-06	up
Hnrnpa3	heterogeneous nuclear ribonucleoprotein A3	5.077	1.59E-07	up
Bub1b	BUB1B, mitotic checkpoint serine/threonine kinase	5.302	1.04E-05	up
Prc1	protein regulator of cytokinesis 1	5.422	7.18E-05	up
Clspn	claspin	5.425	1.42E-04	up
Knstrn	kinetochore-localized astrin/SPAG5 binding	5.650	8.88E-05	up
Foxm1	forkhead box M1	5.708	2.34E-05	up
Kif11	kinesin family member 11	6.347	1.48E-05	up
Fbxo5	F-box protein 5	6.398	3.69E-05	up
Cdca2	cell division cycle associated 2	6.633	6.97E-05	up
Hmmr	hyaluronan mediated motility receptor (RHAMM)	6.938	8.62E-06	up
Spag5	sperm associated antigen 5	7.537	1.44E-04	up
Ckap2	cytoskeleton associated protein 2	7.671	4.25E-05	up
Cdca3	cell division cycle associated 3	7.726	1.04E-04	up
Cdk1	cyclin-dependent kinase 1	7.887	8.26E-07	up
Cip2a	cell proliferation regulating inhibitor protein phosphatase 2A	7.937	7.34E-06	up
Birc5	baculoviral IAP repeat-containing 5	8.057	1.42E-04	up
Kifc1	kinesin family member C1	8.315	6.67E-05	up
Esco2	establishment of sister chromatid cohesion N-acetyltransferase 2	8.408	7.60E-06	up
Diaph3	diaphanous related formin 3	9.062	4.34E-05	up
Ect 2	ect2 oncogene	9.625	9.30E-05	up
Cdca8	cell division cycle associated 8	9.786	1.59E-06	up
Bub1	BUB1, mitotic checkpoint serine/threonine kinase	10.483	8.43E-06	up
Cdkn3	cyclin-dependent kinase inhibitor 3	10.583	1.70E-05	up
Centp	centromere protein E	11.458	1.78E-07	up
Ncapg	non-SMC condensin I complex, subunit G	12.296	2.47E-06	up
Cep 55	centrosomal protein 55	14.075	1.52E-07	up
Mxd3	Max dimerization protein 3	15.098	9.97E-06	up
Sypc2	synaptonemal complex protein 2	440.922	3.66E-05	up
Cd300e	CD300E molecule	1227.930	4.57E-05	up
Adnp	activity-dependent neuroprotective protein	16364.127	8.33E-11	up

### 3.5. GSEA analysis reveals downregulated gene sets in UUO hearts

We performed GSEA analysis of DEGs in UUO hearts using three major pathway databases (GO, KEGG, and Reactome). The top 20 pathways, according to their NES (FDR  $q\text{-val} < 0.25$ ), are shown in Fig. 5A–C. GSEA analysis showed negative gene-set regulation related to mitochondrial oxidative bioenergetic pathways, peroxisomal processes, and autophagy. In UUO hearts, pyruvate metabolism and the tricarboxylic acid cycle, fatty-acid oxidation, glucose metabolism, respiratory electron transport, and branched-chain amino acid catabolism are highly negatively enriched mitochondrial pathways (Fig. 5A–C). Other negatively enriched signaling



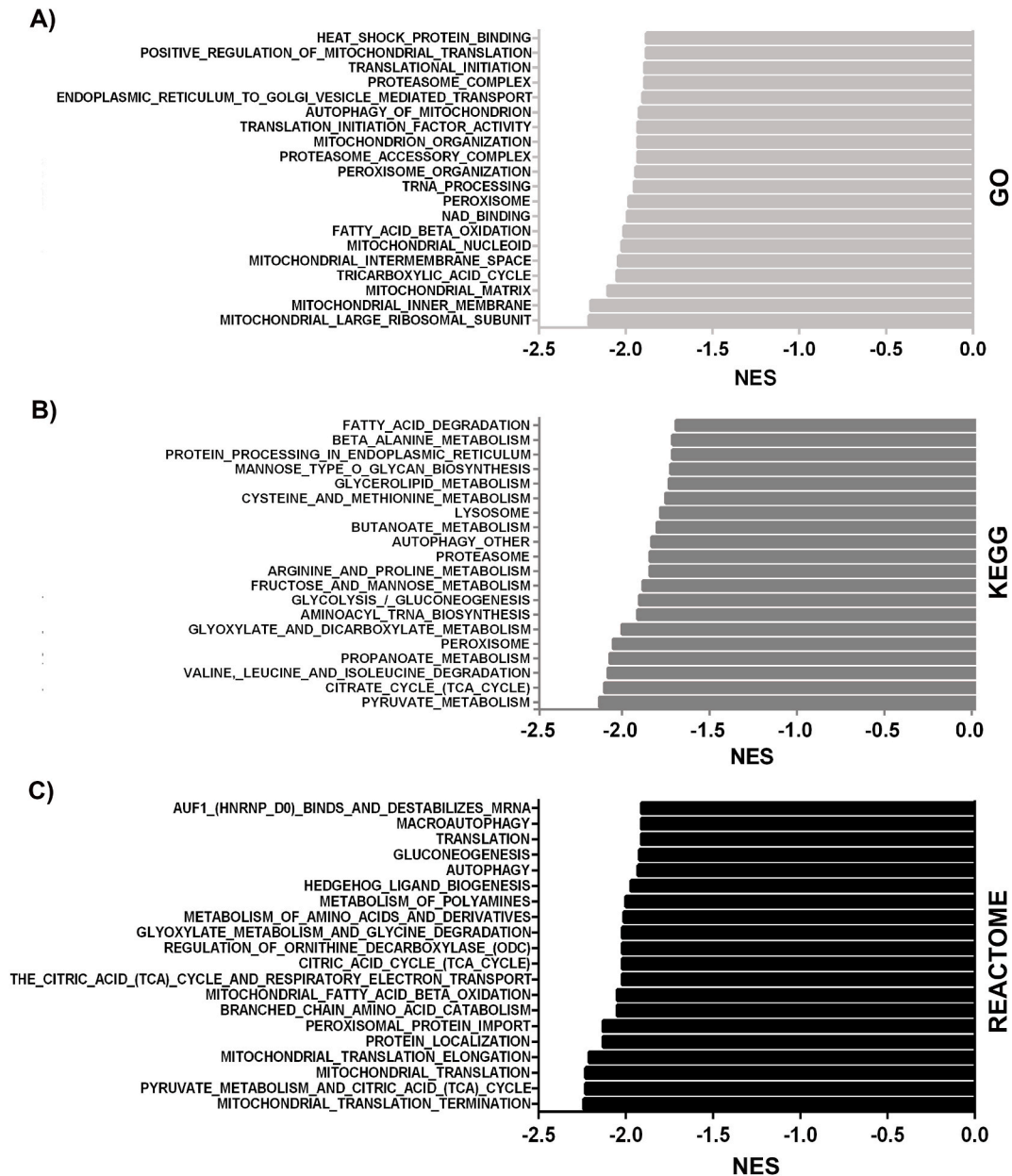


**Fig. 5.** GSEA analysis in UUO hearts. Top 20 negatively enriched pathways (A) GO, (B) KEGG, and (C) REACTOME.  $|NES| \geq 1$ , NOM  $p$ -val < 0.05, and FDR  $q$ -val < 0.25.  $N = 3$ .

#### 4. Discussion

Efforts to understand CVD tend to focus on ESRD patients despite recent evidence pointing to cardiovascular risk increasing earlier within CKD progression, often when sCr is still within normal levels [18]. Here, we used UUO as a mildly uremic model akin to early CKD to study cardiac transcriptional changes involved in developing CRS type 4. UUO results in significant kidney injury, low uremia, pathological cardiac remodeling, and changes in cardiac gene expression.

This study used the same UUO model *Ham O* et al. described as an early-stage, non-uremic, CKD model in C57BL/6 mice that develops cardiac hypertrophy and fibrosis 21 days after UUO [12]. *Ham O* et al. showed a significant increase in sCr (~1.7-fold) and the hypertrophy-associated markers *Anp* and *Bnp* three weeks post-obstruction, which in our hands was not reproducible despite the similarity in surgical procedure, time, and the use of C57BL/6 male mice. However, we did observe significant kidney injury, increased cardiac collagen deposition, and ACTA2 expression. Similar to our findings, *Chen C* et al. demonstrated the presence of myocardial fibrosis in four murine models of uremic cardiomyopathy (pole ligation, 5/6 nephrectomy, unilateral nephrectomy plus contralateral

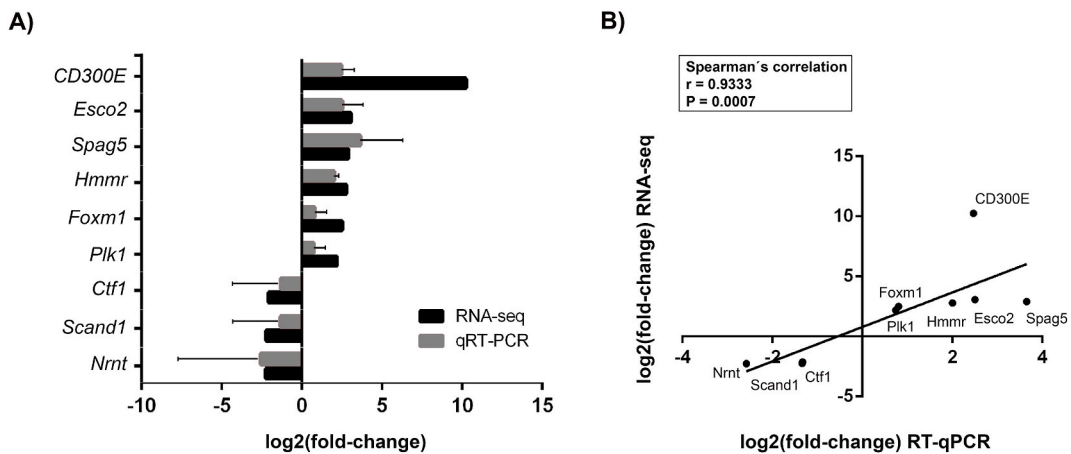


**Fig. 6. RT-qPCR validation.** (A) Log<sub>2</sub> (fold change) expression changes between RNA-seq (N = 3) and RT-qPCR (N = 5) for *CD300E*, *Esco2*, *Spag5*, *Hmmr*, *Foxm1*, *Plk1*, *Ctf1*, *Scand1*, and *Nrnt*. (B) Linear regression plot. The log<sub>2</sub> (fold-change) values for RNA-seq and qRT-PCR are plotted along with the linear fit line. A significant Spearman's correlation coefficient is also shown.

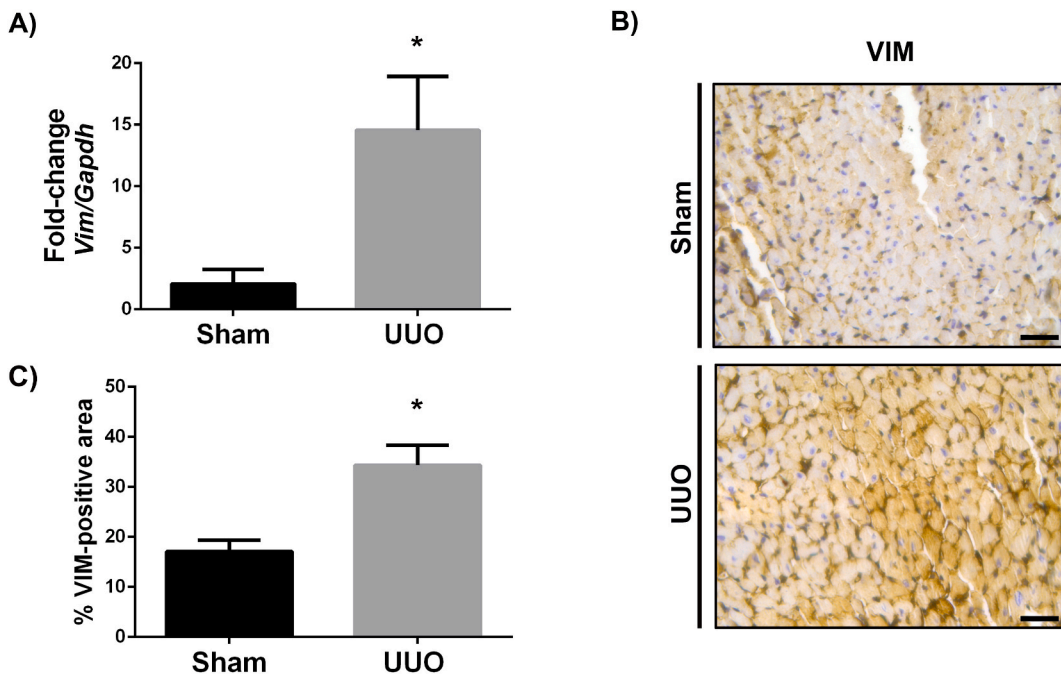


**Fig. 7. Vimentin upregulation in UUO hearts.** (A) *Vim/Gapdh* fold-change by RT-qPCR, \*P < 0.05. (B) Vimentin immunohistochemical detection (400X, scale bar = 100 μm) and (C) quantification. N = 5.

ischemia/reperfusion, and adenine) but were unable to detect increased expression of the hypertrophy biomarkers *Anp* and myosin heavy chain beta [19]. Due to the well-established link between uremia and cardiac hypertrophy markers, we hypothesize that our animals' modest increase in uremia after UUO resulted in lower *Anp* and *Bnp* expression than previously reported [20]. Though the lack of increase in the expression of natriuretic peptides represents a limitation, our results support the suitability of this model at 21 days to study early cardiac remodeling and molecular changes without the burden of severe kidney dysfunction and uremia consistent with the presence of an intact contralateral kidney. More in-depth studies are required to fully understand the time course for renal and cardiac marker expression after UUO.

A decline in renal function promotes angiotensin II and aldosterone production due to sodium and water accumulation, stimulates the calcium-parathyroid axis, and leads to arterial hypertension, all critical risk factors for developing CRS type 4 [1–3]. Even small parathyroid hormone (PTH) increases in CKD patients are associated with an elevated CVD risk independent of calcium, phosphorous, and vitamin D [21]. Hypertension raises cardiac workload, prompting structural and functional changes in the myocardium, including

left ventricle hypertrophy, which can progress to HF [22]. Previous studies in rodents have demonstrated that UUO increases systolic and diastolic blood pressures as soon as two weeks after the intervention [12]. Yet, in several preclinical studies of unilateral UUO, creatinine, phosphorous, PTH, and fibroblast growth factor 23 levels are like control animals despite the confirmed presence of tubular injury [23,24]. Variations in bone mineral metabolism and serum biochemical markers of kidney injury and CVD risk in UUO models have been attributed mainly to the compensatory effect of the contralateral kidney on the excretory function, complicating their reliability at early times. In this study, we did not determine blood pressure, potassium, phosphate, or serum PTH levels. Therefore, we cannot exclude their role in the cardiac transcriptomic changes observed in mice after ureteral obstruction. Nonetheless, we found gene sets associated with the renin-angiotensin system downregulated in UUO hearts.

In UUO hearts, over 80% of DEGs were upregulated. Many were significantly enriched in cell cycle and cell division pathways related to chromatin remodeling (*Adnp*) and cohesin (*Sypc2*, *Ceps5*, *Bub1*, *Esco2*, *Cip2a*, *Cdk1*, *Kif11*, *Clspn*, *Plk1*, *Cdc20*, *Wdhd1*, *Prc1*), a ring-shaped protein complex involved in sister chromatid cohesion in mitosis, DNA replication and repair, genome organization, and gene expression [25,26]. Basal gene expression and myocardial stress-gene responses require a stable yet plastic chromatin architecture [27]. In cardiomyocytes, there is evidence of chromatin architecture reorganization in response to myocardial stress [28]. Moreover, cohesin depletion extensively affects gene expression, and slight decreases in cohesin levels can alter gene regulation without affecting cell division [29]. Although the direct relationship between chromatin architecture and transcriptional effects in this CRS model requires further clarification, our results suggest that early CKD can lead to the onset of extensive transcriptional changes, including the upregulation of multiple genes involved in epigenetic regulation that could drive the development of cardiovascular complications. Yet, whether these changes contribute directly to CRS pathogenesis or occur just as secondary phenomena remain to be addressed through gain- and loss-of-function *in vitro* and *in vivo* experiments of the up- and down-regulated genes.

In this transcriptomic study, we describe an abundance of changes occurring in the heart after UUO that comprise a broad spectrum of biological processes. Among them, we identified other UUO-upregulated cardiac genes (*Birc5*, *Cd300E*, *Foxm1*, *Spag5*, *Hmnr*, *Dach1*, *Akap5*, and *Yes1*) that could advance our understanding of the relationship between kidney disease and cardiac dysfunction due to their involvement in immune responses, cardiac repair, fibrosis, inflammation, proliferation, oxidative stress, and apoptosis [30–33]. These genes could provide novel insights into CKD-related cardiac pathways contributing to CRS progression though their direct contribution needs to be validated experimentally. Importantly, we found differential expression of multiple genes and pathways in the hearts of UUO animals even without significant changes in sCr, further supporting the link between early kidney dysfunction and CVD risk [10,11,18]. Our data suggests that cardiovascular damage at the molecular level starts before traditional biomarkers of CRS can be unequivocally quantified.

The relationship between kidney function and CVD outcomes is less evident in low-risk populations compared to individuals who have some form of CVD or are at high risk for developing CVD [11]. CKD and CRS progression depend on several factors, including genetic background and sex. In animal models of UUO, the C57BL/6 mouse strain develops CKD soon after ureteral obstruction, which does not occur in other mouse strains resistant to CKD, such as BALB/c [34]. Thus, we cannot rule out that our strain choice is associated with a high prevalence of cardiovascular events. Likewise, female mice exhibit tolerance to renal damage in various animal models, and multiple studies have revealed the presence of sexual dimorphisms throughout the Cardiovascular System in health and disease [35–37]. A significant limitation of our study is that we only evaluated transcriptomic changes in male C57BL/6 mice, which introduces bias into our findings. Thus, an evaluation of the DEGs found in this study and their function will need to be further assessed in both sexes to determine their similarities and differences.

Initially, T cell responses promote myocardial healing through fibrosis [38]. Still, when T cell reactivity is sustained, these reparative efforts often result in adverse remodeling that, when chronic, can progress to HF. *Birc5* encodes survivin, a known apoptosis inhibitor that regulates T cell responses identified as a critical gene in the progression of atrial fibrillation [39]. Knockdown or pharmacological inhibition of *Birc5* in T cells attenuates acute allograft rejection survival of cardiac allografts after murine heterotopic heart transplantation by inducing apoptosis [30]. Additionally, targeting *Birc5* through the lncRNA PART1/miR-503-5p pathway prevents apoptosis and improves mitochondrial function in myocardial ischemia-reperfusion injury [40]. Similarly, the myeloid cell surface receptor CD300e fine-tunes immune responses by triggering activation markers expression, releasing proinflammatory cytokines, and regulating T cell-mediated responses [41]. Importantly, focusing on T cells, including Tregs, can be a clue to reveal the reparative mechanism.

The Hippo pathway, a highly conserved signaling pathway that controls organ size, cell proliferation, apoptosis, and differentiation, has emerged as an essential regulator of cardiac development, homeostasis, and regeneration [42]. Moreover, the *Yes1*-associated transcriptional regulator (*Yap1*) leads to myofibroblast activation after myocardial infarction, and YAP1, accompanied by *Foxm1*, participates in various hypertrophic and fibrotic disorders [31]. YAP1 and *Foxm1* upregulation reduces pathological injury in the myocardium [43,44]. In contrast, the cardiac expression of *Yap1* and *Foxm1* increases under hyperglycemic conditions leading to cardiomyocyte hypertrophy and fibrotic responses through increased AKT phosphorylation and Glycogen synthase kinase-3 beta inhibition [31]. FOXM1 also drives TGF- $\beta$ -induced endothelial to mesenchymal transition and, in cardiac endothelial cells, cooperates with the Brahma-related gene-1 (*Brg1*) chromatin remodeler to trigger the angiotensin-converting enzymes pathological switch leading to angiotensin I-to-II conversion and cardiac hypertrophy [45,46]. Additionally, various studies report a cardioprotective role for A-kinase anchoring protein 5 (*Akap5*) by regulating calcineurin, calcium/calmodulin-dependent protein kinase II, and  $\beta$ -adrenergic receptors in the heart [47–49]. Targeting the Hippo pathway, *Foxm1*, and *Akap5* has tremendous potential as a therapeutic strategy for cardiac fibrosis and hypertrophy, with implications for cardiovascular diseases like CRS.

Mitochondrial oxidative bioenergetic pathways, autophagy and peroxisomal pathways were also downregulated in UUO hearts, emphasizing the relevance of mitochondrial dysfunction, homeostasis deregulation, and fatty-acid metabolism alterations in CRS development. Moreover, critical signaling pathways for cardiovascular function like AMPK/mTOR, retinoic acid, HIF-1/VEGF, Hippo,

WNT, and neddylation were also downregulated. These pathways have distinct molecular mechanisms for maintaining cardiac homeostasis and regulating metabolism, autophagy, endoplasmic reticulum stress, fibrosis, organ size, proliferation, regeneration, differentiation, angiogenesis, inflammation, and apoptosis [50–54]. Thus, preclinical studies considering them promising therapeutic targets for cardiovascular therapy could bring new perspectives for CRS treatments.

Furthermore, UO induces cardiac vimentin expression as initially hinted by RNA-seq results (Supplementary file 4), and vimentin has emerged as a myocardial remodeling marker in ischemic heart disease [17]. Although the muscle-specific desmin and laminin are the major intermediate filament proteins linked to cardiomyopathies and HF, we did not find them among the significant DEGs in UO hearts by RNA-seq [55]. For this reason, we decided to evaluate only vimentin expression in our model. Although the role of vimentin in HF and cardiac hypertrophy is not entirely new, our results emphasize the importance of vimentin upregulation in CRS type 4.

CKD disrupts energy equilibrium, immunity, and neuroendocrine signaling and, in consequence, has systemic effects on multiple organs generating complex clinical phenotypes including inflammation, metabolic and nutritional abnormalities, autonomic and central nervous systems dysfunction, and cardiovascular, pulmonary, and bone diseases [56]. In this study, we only evaluated heart tissue, but transcriptomic changes induced by UO probably occur in other organs. Though UO is a widely used model of tubulointerstitial kidney fibrosis, multiple studies have reported changes in lung function, bone metabolism and structure, and cognitive and neuropathological damage following obstructive nephropathy [57–59]. Hence, the global changes occurring after UO cannot be underestimated but instead studied further to understand and treat better the systemic complications of renal diseases.

In this study, we performed irreversible, unilateral UO in which the left ureter was ligated and cut to induce hydronephrosis, severe inflammation, and interstitial scarring over 21 days as a model of early CKD. However, acute kidney injury secondary to obstructive nephropathy is frequent, impacting the morbidity and mortality of affected patients [60]. Thus, using UO models in which the ureteric obstruction is surgically reversed (r-UO) allows for kidney decompression and urinary flow restoration to the bladder while providing the opportunity to study the resolution of inflammation and tissue repair [34,61]. It is unclear whether removing the harmful stimulus at different times after ureteral obstruction could restore the DEGs in UO hearts to Sham levels, mainly since there is evidence that relieving the urinary tract cannot fully recover kidney function and has residual impairments that can lead to ESRD [14]. Still, using r-UO models in the future could be helpful to determine how the heart recovers after an acute kidney injury event.

Transcriptomic data from the whole heart is representative of changes occurring across all cell types, thus presenting a limitation of this study. More detailed, single-cell transcriptomic studies are needed to discover differences at the cellular level that the heterogeneity of the heart could be masking. Still, our results suggest that CRS type 4 development involves global transcriptional changes and highlight the importance of understanding the molecular mechanisms driving CVD risk at early points during renal disease progression.

## 5. Conclusions

This study identified novel pathways involved in the pathogenesis of CRS type 4 by investigating the cardiac transcriptomic changes in an early-stage CKD murine model induced by UO. Our results suggest that early CKD can lead to the onset of widespread transcriptional changes implicated in CVD development. In UO hearts, over 80% of DEGs were upregulated and enriched in cell cycle and cell division pathways related to chromatin remodeling, immune responses, cardiac repair, fibrosis, inflammation, proliferation, oxidative stress, and apoptosis. Interestingly, mitochondrial oxidative bioenergetic pathways, autophagy and peroxisomal pathways were downregulated in UO hearts, emphasizing the role of altered mitochondrial function, homeostasis, and fatty-acid metabolism in the development of CRS type 4.

### Institutional review board statement

The Local Health Research Committee of CIBO, IMSS (CLIES R-2021-1305-013) approved all the procedures.

### Informed consent statement

Not applicable.

### Data availability statement

The data that support the findings of this study are openly available in NCBI GEO repository under accession code GSE235751 and within the article's supplementary materials.

### CRedit authorship contribution statement

**Francisco Javier Munguia-Galaviz:** Conceptualization, Formal analysis, Investigation. **Yanet Karina Gutierrez-Mercado:** Investigation, Resources. **Alejandra Guillermina Miranda-Diaz:** Conceptualization, Writing – review & editing. **Eliseo Portilla de Buen:** Writing – review & editing. **Mario Eduardo Flores-Soto:** Resources. **Raquel Echavarría:** Conceptualization, Formal analysis, Investigation, Writing – original draft.

## Declaration of competing interest

The authors declare that they have no known competing financial interests or personal relationships that could have appeared to influence the work reported in this paper.

## Acknowledgements

The graphical abstract was created with [biorender.com](https://biorender.com).

## Appendix A. Supplementary data

Supplementary data to this article can be found online at <https://doi.org/10.1016/j.heliyon.2024.e27468>.

## References

- [1] J. Rangaswami, V. Bhalla, J.E.A. Blair, T.I. Chang, S. Costa, K.L. Lentine, E.V. Lerma, K. Mezue, M. Molitch, W. Mullens, C. Ronco, W.H.W. Tang, P. A. McCullough, American Heart Association Council on the Kidney in Cardiovascular D, Council on Clinical C, Cardiorenal syndrome: Classification, pathophysiology, diagnosis, and treatment Strategies: a scientific statement from the American heart association, *Circulation* 139 (16) (2019) e840–e878, <https://doi.org/10.1161/CIR.0000000000000664>.
- [2] A. Clementi, G.M. Virzi, C.Y. Goh, D.N. Cruz, A. Granata, G. Vescovo, C. Ronco, Cardiorenal syndrome type 4: a review, *Cardiorenal Med.* 3 (1) (2013) 63–70, <https://doi.org/10.1159/000350397>.
- [3] P. Hatamizadeh, G.C. Fonarow, M.J. Budoff, S. Darabian, C.P. Kovesdy, K. Kalantar-Zadeh, Cardiorenal syndrome: pathophysiology and potential targets for clinical management, *Nat. Rev. Nephrol.* 9 (2) (2013) 99–111, <https://doi.org/10.1038/nrneph.2012.279>.
- [4] C.P. Kovesdy, Epidemiology of chronic kidney disease: an update 2022, *Kidney Int. Suppl.* 12 (1) (2022) 7–11, <https://doi.org/10.1016/j.kisu.2021.11.003>.
- [5] J. Jankowski, J. Floege, D. Fliser, M. Bohm, N. Marx, Cardiovascular disease in chronic kidney disease: pathophysiological insights and therapeutic options, *Circulation* 143 (11) (2021) 1157–1172, <https://doi.org/10.1161/CIRCULATIONAHA.120.050686>.
- [6] L. Di Lullo, A. Gorini, D. Russo, A. Santoboni, C. Ronco, Left ventricular hypertrophy in chronic kidney disease patients: from pathophysiology to treatment, *Cardiorenal Med.* 5 (4) (2015) 254–266, <https://doi.org/10.1159/000435838>.
- [7] C. Tuegel, N. Bansal, Heart failure in patients with kidney disease, *Heart* 103 (23) (2017) 1848–1853, <https://doi.org/10.1136/heartjnl-2016-310794>.
- [8] A. Minciunescu, L. Genovese, C. deFilippi, Cardiovascular alterations and structural changes in the setting of chronic kidney disease: a review of cardiorenal syndrome type 4, *SN Compr Clin Med* 5 (1) (2023) 15, <https://doi.org/10.1007/s42399-022-01347-2>.
- [9] P.G. de Albuquerque Suassuna, H. Sanders-Pinheiro, R.B. de Paula, Uremic cardiomyopathy: a new piece in the chronic kidney disease-mineral and bone disorder puzzle, *Front. Med.* 5 (2018) 206, <https://doi.org/10.3389/fmed.2018.00206>.
- [10] S. Lai, M. Dimko, A. Galani, B. Coppola, G. Innico, N. Frassetto, E.D. Mazzei, A. Mariotti, Early markers of cardiovascular risk in chronic kidney disease, *Ren. Fail.* 37 (2) (2015) 254–261, <https://doi.org/10.3109/0886022X.2014.982489>.
- [11] L. Zhang, L. Zuo, F. Wang, M. Wang, S. Wang, J. Lv, L. Liu, H. Wang, Cardiovascular disease in early stages of chronic kidney disease in a Chinese population, *J. Am. Soc. Nephrol.* 17 (9) (2006) 2617–2621, <https://doi.org/10.1681/ASN.2006040402>.
- [12] O. Ham, W. Jin, L. Lei, H.H. Huang, K. Tsuji, M. Huang, J. Roh, A. Rosenzweig, H.A.J. Lu, Pathological cardiac remodeling occurs early in CKD mice from unilateral urinary obstruction, and is attenuated by Enalapril, *Sci. Rep.* 8 (1) (2018) 16087, <https://doi.org/10.1038/s41598-018-34216-x>.
- [13] S. Chinnappa, E. White, N. Lewis, O. Baldo, Y.K. Tu, G. Glorieux, R. Vanholder, M. El Nahas, A. Mooney, Early and asymptomatic cardiac dysfunction in chronic kidney disease, *Nephrol. Dial. Transplant.* 33 (3) (2018) 450–458, <https://doi.org/10.1093/ndt/gfx064>.
- [14] E.E. Hesketh, M.A. Vernon, P. Ding, S. Clay, G. Borthwick, B. Conway, J. Hughes, A murine model of irreversible and reversible unilateral ureteric obstruction, *J. Vis. Exp.* 94 (2014), <https://doi.org/10.3791/52559>.
- [15] A. Subramanian, P. Tamayo, V.K. Mootha, S. Mukherjee, B.L. Ebert, M.A. Gillette, A. Paulovich, S.L. Pomeroy, T.R. Golub, E.S. Lander, J.P. Mesirov, Gene set enrichment analysis: a knowledge-based approach for interpreting genome-wide expression profiles, *Proc Natl Acad Sci U S A* 102 (43) (2005) 15545–15550, <https://doi.org/10.1073/pnas.0506580102>.
- [16] Y. Chang, Y. Ben, H. Li, Y. Xiong, G. Chen, J. Hao, X. Ma, X. Gao, P. Qiang, T. Shimosawa, X. Wang, F. Yang, Q. Xu, Eplerenone prevents cardiac fibrosis by inhibiting angiogenesis in unilateral urinary obstruction rats, *J Renin Angiotensin Aldosterone Syst* 2022 (2022) 1283729, <https://doi.org/10.1155/2022/1283729>.
- [17] T. Kondo, M. Takahashi, G. Yamasaki, M. Sugimoto, A. Kuse, M. Morichika, K. Nakagawa, M. Sakurada, M. Asano, Y. Ueno, Immunohistochemical analysis of vimentin expression in myocardial tissue from autopsy cases of ischemic heart disease, *Leg. Med.* 54 (2022) 102003, <https://doi.org/10.1016/j.legalmed.2021.102003>.
- [18] N.C. Edwards, W.E. Moody, C.D. Chue, C.J. Ferro, J.N. Townsend, R.P. Steeds, Defining the natural history of uremic cardiomyopathy in chronic kidney disease: the role of cardiovascular magnetic resonance, *JACC Cardiovasc Imaging* 7 (7) (2014) 703–714, <https://doi.org/10.1016/j.jcmg.2013.09.025>.
- [19] C. Chen, C. Xie, H. Wu, L. Wu, J. Zhu, H. Mao, C. Xing, Uraemic cardiomyopathy in different mouse models, *Front. Med.* 8 (2021) 690517, <https://doi.org/10.3389/fmed.2021.690517>.
- [20] M. Codognotto, A. Piccoli, M. Zaninotto, M. Mion, M. Plebani, U. Vertolli, F. Tona, L. Ruzza, A. Barchita, G.M. Boffa, Renal dysfunction is a confounder for plasma natriuretic peptides in detecting heart dysfunction in uremic and idiopathic dilated cardiomyopathies, *Clin. Chem.* 53 (12) (2007) 2097–2104, <https://doi.org/10.1373/clinchem.2007.089656>.
- [21] G. Pontoriero, M. Cozzolino, F. Locatelli, D. Braccaccio, CKD patients: the dilemma of serum PTH levels, *Nephron Clin. Pract.* 116 (4) (2010) c263–c268, <https://doi.org/10.1159/000318787>.
- [22] S. Saheera, P. Krishnamurthy, Cardiovascular changes associated with hypertensive heart disease and aging, *Cell Transplant.* 29 (2020) 963689720920830, <https://doi.org/10.1177/0963689720920830>.
- [23] X. Zhang, T. Li, L. Wang, Y. Li, T. Ruan, X. Guo, Q. Wang, X. Meng, Relative comparison of chronic kidney disease-mineral and bone disorder rat models, *Front. Physiol.* 14 (2023) 1083725, <https://doi.org/10.3389/fphys.2023.1083725>.
- [24] E.R. Smith, S.J. Tan, S.G. Holt, T.D. Hewitson, FGF23 is synthesised locally by renal tubules and activates injury-primed fibroblasts, *Sci. Rep.* 7 (1) (2017) 3345, <https://doi.org/10.1038/s41598-017-02709-w>.
- [25] J.A. Horsfield, Full circle: a brief history of cohesin and the regulation of gene expression, *FEBS J.* 290 (7) (2023) 1670–1687, <https://doi.org/10.1111/febs.16362>.
- [26] X. Sun, W. Yu, L. Li, Y. Sun, ADNP controls gene expression through local chromatin architecture by association with BRG1 and CHD4, *Front. Cell Dev. Biol.* 8 (2020) 553, <https://doi.org/10.3389/fcell.2020.00553>.

- [27] D.P. Lee, W.L.W. Tan, C.G. Anene-Nzelu, C.J.M. Lee, P.Y. Li, T.D.A. Luu, C.X. Chan, Z. Tiang, S.L. Ng, X. Huang, M. Efthymios, M.I. Autio, J. Jiang, M. J. Fullwood, S. Prabhakar, E. Lieberman Aiden, R.S. Foo, Robust CTCF-based chromatin architecture underpins epigenetic changes in the heart failure stress-gene response, *Circulation* 139 (16) (2019) 1937–1956, <https://doi.org/10.1161/CIRCULATIONAHA.118.036726>.
- [28] M. Rosa-Garrido, D.J. Chapski, A.D. Schmitt, T.H. Kimball, E. Karbassi, E. Monte, E. Balderas, M. Pellegrini, T.T. Shih, E. Soehalim, D. Liem, P. Ping, N.J. Galjart, S. Ren, Y. Wang, B. Ren, T.M. Vondriska, High-resolution mapping of chromatin conformation in cardiac myocytes reveals structural remodeling of the epigenome in heart failure, *Circulation* 136 (17) (2017) 1613–1625, <https://doi.org/10.1161/CIRCULATIONAHA.117.029430>.
- [29] J.A. Horsfield, S.H. Anagnostou, J.K. Hu, K.H. Cho, R. Geisler, G. Lieschke, K.E. Crosier, P.S. Crosier, Cohesin-dependent regulation of Runx genes, *Development* 134 (14) (2007) 2639–2649, <https://doi.org/10.1242/dev.002485>.
- [30] H. Xu, J. Yu, J. Cui, Z. Chen, X. Zhang, Y. Zou, Y. Du, Y. Li, S. Le, L. Jiang, J. Xia, J. Wu, Ablation of survivin in T cells attenuates acute allograft rejection after murine heterotopic heart transplantation by inducing apoptosis, *Front. Immunol.* 12 (2021) 710904, <https://doi.org/10.3389/fimmu.2021.710904>.
- [31] A. Mondal, S. Das, J. Samanta, S. Chakraborty, A. Sengupta, YAP1 induces hyperglycemic stress-mediated cardiac hypertrophy and fibrosis in an AKT-FOXM1 dependent signaling pathway, *Arch. Biochem. Biophys.* 722 (2022) 109198, <https://doi.org/10.1016/j.abb.2022.109198>.
- [32] Q. Chen, Y. Tang, H. Deng, B. Liang, H. Li, Z. Li, H. Zhu, L. Chen, Curcumin improves keratinocyte proliferation, inflammation, and oxidative stress through mediating the SPAG5/FOXM1 Axis in an in vitro model of actinic dermatitis by ultraviolet, *Dis. Markers* 2022 (2022) 5085183, <https://doi.org/10.1155/2022/5085183>.
- [33] Z. Wang, X. Zhang, F. Zhu, S. Zhou, Q. Wang, H. Wang, A-kinase anchoring protein 5 anchors protein kinase A to mediate PLN/SERCA to reduce cardiomyocyte apoptosis induced by hypoxia and reoxygenation, *Biochem. Cell. Biol.* 100 (2) (2022) 162–170, <https://doi.org/10.1139/bcb-2021-0466>.
- [34] T.S. Puri, M.I. Shakaib, A. Chang, L. Mathew, O. Olayinka, A.W. Minto, M. Sarav, B.K. Hack, R.J. Quigg, Chronic kidney disease induced in mice by reversible unilateral ureteral obstruction is dependent on genetic background, *Am J Physiol Renal Physiol* 298 (4) (2010) F1024–F1032, <https://doi.org/10.1152/ajprenal.00384.2009>.
- [35] Z. Melo, Y.K. Gutierrez-Mercado, D. Garcia-Martinez, E. Portilla-de-Buen, A.A. Canales-Aguirre, R. Gonzalez-Gonzalez, A. Franco-Acevedo, J. Palomino, R. Echavarría, Sex-dependent mechanisms involved in renal tolerance to ischemia-reperfusion: role of inflammation and histone H3 citrullination, *Transpl. Immunol.* 63 (2020) 101331, <https://doi.org/10.1016/j.trim.2020.101331>.
- [36] C.S.P. Lam, C. Arnott, A.L. Beale, C. Chandramouli, D. Hilfiker-Kleiner, D.M. Kaye, B. Ky, B.T. Santema, K. Sliwa, A.A. Voors, Sex differences in heart failure, *Eur. Heart J.* 40 (47) (2019) 3859–3868, <https://doi.org/10.1093/eurheartj/ehz835>.
- [37] L.A. Leinwand, Sex is a potent modifier of the cardiovascular system, *J. Clin. Invest.* 112 (3) (2003) 302–307, <https://doi.org/10.1172/JCI19429>.
- [38] T. Kino, M. Khan, S. Mohsin, The regulatory role of T cell responses in cardiac remodeling following myocardial infarction, *Int. J. Mol. Sci.* 21 (14) (2020), <https://doi.org/10.3390/ijms21145013>.
- [39] Z. Zhao, G. Liu, H. Zhang, P. Ruan, J. Ge, Q. Liu, BIRC5, GAJ5, and lncRNA NPHP3-AS1 are correlated with the development of atrial fibrillation-valvular heart disease, *Int. Heart J.* 62 (1) (2021) 153–161, <https://doi.org/10.1536/ihj.20-238>.
- [40] Z. Guo, M. Zhao, G. Jia, R. Ma, M. Li, LncRNA PART1 alleviated myocardial ischemia/reperfusion injury via suppressing miR-503-5p/BIRC5 mediated mitochondrial apoptosis, *Int. J. Cardiol.* 338 (2021) 176–184, <https://doi.org/10.1016/j.ijcard.2021.05.044>.
- [41] S. Coletta, V. Salvi, C. Della Bella, A. Bertocco, S. Lonardi, E. Trevellin, M. Fassan, M.M. D'Ellos, W. Vermi, R. Vettor, S. Cagnin, S. Sozzani, G. Codolo, M. de Bernard, The immune receptor CD300e negatively regulates T cell activation by impairing the STAT1-dependent antigen presentation, *Sci. Rep.* 10 (1) (2020) 16501, <https://doi.org/10.1038/s41598-020-73552-9>.
- [42] F. Meng, B. Xie, J.F. Martin, Targeting the Hippo pathway in heart repair, *Cardiovasc. Res.* 118 (11) (2022) 2402–2414, <https://doi.org/10.1093/cvr/cvab291>.
- [43] S. Song, Y. Wang, H.Y. Wang, L.L. Guo, Role of sevoflurane in myocardial ischemia-reperfusion injury via the ubiquitin-specific protease 22/lysine-specific demethylase 3A axis, *Bioengineered* 13 (5) (2022) 13366–13383, <https://doi.org/10.1080/21655979.2022.2062535>.
- [44] G. Zhang, K. Yu, Z. Bao, X. Sun, D. Zhang, Upregulation of FoxM1 protects against ischemia/reperfusion-induced myocardial injury, *Acta Biochim. Pol.* 68 (4) (2021) 653–658, <https://doi.org/10.18388/abp.2020.5536>.
- [45] S. Song, R. Zhang, W. Cao, G. Fang, Y. Yu, Y. Wan, C. Wang, Y. Li, Q. Wang, Foxm1 is a critical driver of TGF-beta-induced EndMT in endothelial cells through Smad2/3 and binds to the Snail promoter, *J. Cell. Physiol.* 234 (6) (2019) 9052–9064, <https://doi.org/10.1002/jcp.27583>.
- [46] J. Yang, X. Feng, Q. Zhou, W. Cheng, C. Shang, P. Han, C.H. Lin, H.S. Chen, T. Quertermous, C.P. Chang, Pathological Ace2-to-Ace enzyme switch in the stressed heart is transcriptionally controlled by the endothelial Brg1-FoxM1 complex, *Proc Natl Acad Sci U S A* 113 (38) (2016) E5628–E5635, <https://doi.org/10.1073/pnas.1525078113>.
- [47] F. Zhu, Q. Wang, Z. Wang, X. Zhang, B. Zhang, H. Wang, Metoprolol mitigates ischemic heart remodeling and fibrosis by increasing the expression of AKAP5 in ischemic heart, *Oxid. Med. Cell. Longev.* 2022 (2022) 5993459, <https://doi.org/10.1155/2022/5993459>.
- [48] X. Zhang, Q. Wang, Z. Wang, H. Zhang, F. Zhu, J. Ma, W. Wang, Z. Chen, H. Wang, Interaction between A-kinase anchoring protein 5 and protein kinase A mediates CaMKII/HDAC signaling to inhibit cardiomyocyte hypertrophy after hypoxic reoxygenation, *Cell. Signal.* 103 (2023) 110569, <https://doi.org/10.1016/j.cellsig.2022.110569>.
- [49] X. Li, S.M. Matta, R.D. Sullivan, S.W. Bahouth, Carvedilol reverses cardiac insufficiency in AKAP5 knockout mice by normalizing the activities of calcineurin and CaMKII, *Cardiovasc. Res.* 104 (2) (2014) 270–279, <https://doi.org/10.1093/cvr/cvu209>.
- [50] X. Li, J. Liu, Q. Lu, D. Ren, X. Sun, T. Rousselet, Y. Tan, J. Li, AMPK: a therapeutic target of heart failure—not only metabolism regulation, *Biosci. Rep.* 39 (1) (2019), <https://doi.org/10.1042/BSR20181767>.
- [51] K.A. Hemanthakumar, R. Kivela, Angiogenesis and angiocrines regulating heart growth, *Vasc Biol* 2 (1) (2020) R93–R104, <https://doi.org/10.1530/VB-20-0006>.
- [52] J. Xie, Y. Wang, D. Ai, L. Yao, H. Jiang, The role of the Hippo pathway in heart disease, *FEBS J.* 289 (19) (2022) 5819–5833, <https://doi.org/10.1111/febs.16092>.
- [53] Y. Zhao, C. Wang, X. Hong, J. Miao, Y. Liao, F.F. Hou, L. Zhou, Y. Liu, Wnt/beta-catenin signaling mediates both heart and kidney injury in type 2 cardiorenal syndrome, *Kidney Int.* 95 (4) (2019) 815–829, <https://doi.org/10.1016/j.kint.2018.11.021>.
- [54] J. Li, J. Zou, R. Littlejohn, J. Liu, H. Su, Neddylation, an emerging mechanism regulating cardiac development and function, *Front. Physiol.* 11 (2020) 612927, <https://doi.org/10.3389/fphys.2020.612927>.
- [55] M. Tsikitis, Z. Galata, M. Mavroidis, S. Psarras, Y. Capetanaki, Intermediate filaments in cardiomyopathy, *Biophys Rev* 10 (4) (2018) 1007–1031, <https://doi.org/10.1007/s12551-018-0443-2>.
- [56] C. Zoccali, R. Vanholder, Z.A. Massy, A. Ortiz, P. Sarafidis, F.W. Dekker, D. Fliser, D. Fouque, G.H. Heine, K.J. Jager, M. Kanbay, F. Mallamaci, G. Parati, P. Rossignol, A. Wiecek, G. London, R. European, Cardiovascular Medicine Working Group of the European Renal Association - European Dialysis Transplantation A, The systemic nature of CKD, *Nat. Rev. Nephrol.* 13 (6) (2017) 344–358, <https://doi.org/10.1038/nrneph.2017.52>.
- [57] F. Yang, Y. Chang, C. Zhang, Y. Xiong, X. Wang, X. Ma, Z. Wang, H. Li, T. Shimosawa, L. Pei, Q. Xu, UUU induces lung fibrosis with macrophage-myofibroblast transition in rats, *Int Immunopharmacol* 93 (2021) 107396, <https://doi.org/10.1016/j.intimp.2021.107396>.
- [58] S.S. Gu, Y. Zhang, X. Chen, T.Y. Diao, Y. Geburu, M.S. Wong, Trabecular bone deterioration at the greater trochanter of mice with unilateral obstructive nephropathy, *Asian J. Androl.* 15 (4) (2013) 564–566, <https://doi.org/10.1038/aja.2013.34>.
- [59] Y.S. Ho, C.F. Lau, K. Lee, J.Y. Tan, J. Lee, S. Yung, R.C. Chang, Impact of unilateral ureteral obstruction on cognition and neurodegeneration, *Brain Res. Bull.* 169 (2021) 112–127, <https://doi.org/10.1016/j.brainresbull.2021.01.001>.
- [60] J.S. Chavez-Iniguez, G.J. Navarro-Gallardo, R. Medina-Gonzalez, L. Alcantar-Vallin, G. Garcia-Garcia, Acute kidney injury caused by obstructive nephropathy, *Int J Nephrol* 2020 (2020) 8846622, <https://doi.org/10.1155/2020/8846622>.
- [61] A. Narvaez Barros, R. Guiteras, A. Sola, A. Manonelles, J. Morote, J.M. Cruzado, Reversal unilateral ureteral obstruction: a mice experimental model, *Nephron* 142 (2) (2019) 125–134, <https://doi.org/10.1159/000497119>.